Article

A Conflict Evidence Fusion Method Based on Bray–Curtis Dissimilarity and the Belief Entropy

Yue Liu [1,2], Tianji Zou [1,2] and Hongyong Fu [1,*]

1   Key Laboratory of Space Utilization, Technology and Engineering Center for Space Utilization, Chinese Academy of Sciences, Beijing 100094, China; liuyue22@csu.ac.cn (Y.L.); zoutianji@csu.ac.cn (T.Z.)
2   School of Aeronautics and Astronautics, University of Chinese Academy of Sciences, Beijing 100049, China
*   Correspondence: fuhongyong@csu.ac.cn; Tel.: +86-186-0000-5286

Abstract: The D-S evidence theory is extensively applied to manage uncertain information. However, the theory encounters challenges related to conflicts during the fusion process, impeding the precise identification of multi-subset focal elements. This paper introduces a novel method for conflicting evidence fusion that incorporates the Bray–Curtis dissimilarity, cosine distance of the included angle, and belief entropy. The method comprehensively evaluates three aspects—evidence similarity, evidence distance, and the amount of information—while considering factors like the credibility and uncertainty of evidence. Initially, the evidence undergoes conversion into single-subset focal element evidence through the improved Pignistic probability function. Subsequently, the credibility between pieces of evidence is established using the Bray–Curtis dissimilarity and angle cosine distance, while the uncertainty of the evidence is computed using belief entropy. The weighted correction coefficient of the evidence is determined by integrating the credibility and uncertainty of the evidence. Subsequently, the corrected evidence is fused using the D-S evidence theory to derive the final judgment. An analysis of two sets of arithmetic examples, considering both single-subset and multi-subset focal elements, demonstrates the faster convergence and enhanced accuracy and reliability of the proposed method in comparison to existing approaches.

Keywords: D-S evidence theory; Bray–Curtis dissimilarity; belief entropy; improved Pignistic probability function; cosine of included angle

1. Introduction

The Dempster–Shafer (D-S) evidence theory [1] is an uncertainty reasoning method first proposed by Dempster in 1967 and later refined by his student Shafer [2]. The D-S evidence theory is adept at characterizing and expressing uncertain information in scenarios where a priori probabilities are lacking. Consequently, it finds extensive application in the fields of multi-sensor information fusion [3,4], classification [5,6], fault diagnosis [7,8], decision making [9,10], and state assessment [11,12]. Despite its widespread utility, it encounters some difficulties. For example, evidence theory faces challenges when fusing conflicting evidence from multiple sources, giving rise to common issues such as the common problems of complete conflict paradox, 0-trust paradox, 1-trust paradox, and high-conflict paradox [13].

Currently, there are two main ideas to address the deficiency of the D-S theory of evidence in dealing with conflicting evidence. The first is to modify the synthesis rules of the evidence theory [14]. For example, Yager [15] proposed to assign all of the conflicting information to the uncertainty domain. Florea [16] introduced a class of robust combination rules (RCR) in which the weights are a function of the conflict between two pieces of information that automatically consider the reliability of information sources. Su [17] presented an improved evidence fusion rule based on the concept of joint belief distribution.

By modifying the synthesis rules, although it solves the problem of the fusion of conflicting evidence to a certain extent, it destroys the excellent exchange law, combination

law, and other mathematical properties of the D-S evidence theory, and it is less effective in fusing a large amount of evidence, which has certain limitations. To minimize conflicts, the second approach is to modify the weight coefficients of conflicting evidence and reduce the degree of conflict of evidence; this method will not change the excellent properties of the D-S evidence theory, which has received more attention from scholars. For instance, Murphy [18] proposed the average weighting method of evidence, assigning equal weight to each piece of evidence. However, this method overlooks the correlation between pieces of evidence, resulting in poorer fusion result accuracy. Deng [19] introduced a method to quantify the degree of conflict between the evidence based on the Jousselme distance and subsequently determine the weighting coefficients of the evidence, which compensates for the shortcomings of the average weighting method to a certain extent. Lin [20] presented an evidence fusion method based on the Mahalanobis distance, enhancing the accuracy of conflicting evidence fusion. Shi [21] proposed an evidence combination method based on Manhattan distance and evidence angle. Tang [22] proposed a conflict evidence fusion method based on correlation coefficients in complex networks. This innovative approach leverages interactive relationships between bodies of evidence to depict correlation coefficients, adjusting the weights of conflicting evidence accordingly. Chen [7] proposed a weighted correction method based on the Jousselme distance and uncertainty measures, demonstrating enhanced accuracy compared with relying solely on distance for conflict coefficient correction and exhibiting improved convergence properties. Xiao [23] introduced a multi-sensor data fusion method grounded in plausibility dispersion measure and belief entropy. This method employs Jensen–Shannon dispersion to quantify conflict between evidences, combines it with Deng entropy to assess uncertainty, and consequently corrects plausibility. Zhao [24] presented a novel multi-sensor evidence fusion algorithm based on the square-mean distribution distance, integrating it with entropy to enhance the fusion accuracy of conflicting evidence. Li [25] proposed a weighted conflicting evidence combination method using Hellinger distance and belief entropy. These metrics construct weight coefficients for the evidence subsequently applied to weight the original evidence. Wang [26] suggested a conflict evidence fusion method based on Lance distance and credibility entropy, accounting for credibility and uncertainty to measure the discount coefficient for the final evidence fusion, thereby correcting the original evidence. Zhou [27] introduced the cosine of the angle to gauge the degree of conflict between evidence, correcting the conflict coefficient. This method constructs judgment rules for evidence grouping by utilizing a combination of the conflict coefficient and belief entropy. The resulting coefficient is then applied to weigh the original evidence, amending it effectively for a single subset of evidence conflict fusion.

In summary, the primary approach to addressing the conflict problem is correcting the weight coefficients of evidence sources. Generally, entropy is employed to describe the uncertainty of the evidence itself, while the correlation between evidence is captured through conflict coefficients such as the conflict coefficient k, Jousselme distance, Hellinger distance, Lance distance, Mahalanobis distance, and so on. Simultaneously considering the correlation and uncertainty of the evidence yields correction coefficients, ultimately enhancing the accuracy of fusion results.

However, the majority of the aforementioned scholars' research focuses on conflicting evidence within single-subset focal elements, leaving the conflict problem of multi-subset focal elements unresolved. To address these prevailing issues, a comprehensive solution is proposed, introducing an enhanced Pignistic probability function. This function allocates multi-subset focal element evidence into single-subset focal element evidence, effectively resolving both single-subset and multi-subset focal element conflict problems. Additionally, the Jousselme distance is influenced by the dispersion degree of the basic trust allocation function of the evidence, potentially yielding results contrary to reality when measuring evidence conflict. The Mahalanobis distance necessitates covariance calculation, and the process of computing squared mean is intricate, making it unsuitable for large-scale data processing.

Consequently, this paper advocates a more optimal measure—the Bray–Curtis dissimilarity. This measure adheres to the principles of non-negativity, symmetry and normality, aligning with the requirements of the D-S evidence theory. The Bray–Curtis dissimilarity is a non-parametric metric that avoids the need for assumptions or parameterization of probability distributions, rendering it applicable to various types of uncertainty distributions without being constrained by specific assumptions. This similarity metric demonstrates adaptability in scenarios where data may include missing values or an unequal number of data points. In practical applications, the reliability and completeness of evidence may vary, and the Bray–Curtis dissimilarity provides a relatively flexible approach under such circumstances. Furthermore, the computation of the Bray–Curtis dissimilarity is straightforward, making it suitable for large-scale data processing. Its simplicity facilitates implementation and comprehension, contributing to its practical utility in diverse research contexts.

To tackle the challenge of evidence conflict fusion, a multi-step approach is employed. Firstly, leveraging the weights in the basic probability function, an improved Pignistic probability function is applied to allocate multi-subset focal element evidence to single-subset focal element evidence. This step aims to reduce computational complexity and minimize information loss during the conversion process. Secondly, a novel method is introduced to calculate conflict coefficients between evidences based on the Bray–Curtis dissimilarity. The Bray–Curtis dissimilarity, in combination with the cosine of included angle distance, is employed to gauge the degree of conflict and discrepancy among the evidence. Subsequently, belief entropy is used to quantify evidence uncertainty, and these three influencing factors are amalgamated to derive corresponding weighted correction coefficients. These coefficients are then applied to weight and correct the original evidence. Finally, the D-S evidence theory is employed to fuse the updated evidence sources. The validation of two conflicting evidence algorithms, incorporating both single-subset and multi-subset focal elements, demonstrates improved convergence and robustness compared to previous methods.

2. Preliminaries

In this section, the pertinent theoretical foundations of the D-S theory of evidence will be given in detail.

2.1. The Frame of Discernment

In the D-S evidence theory [28–31], the process of evidence reasoning is grounded in a sample space consisting of non-empty finite sets, referred to as the identification frame Θ. If $\Theta = \{A_1, A_2, \cdots, A_i\}$, where A_i is a subset of the identification frame Θ, then the subsets within Θ are mutually exclusive pairwise.

It is customary to represent the power set of the recognition frame Θ. Denoted as 2^{Θ}, it encompasses all subsets in Θ, including the empty set and Θ itself, expressed as follows:

$$2^{\Theta} = \{\varnothing, \{A_1\}, \cdots, \{A_n\}, \{A_1, A_2\}, \cdots, \{A_1, A_2, A_3\}, \cdots, \Theta\}.$$

Here, $\varnothing$ signifies the empty set, $\{A_1, A_2\}$ represents $\{A_1 \cap A_2\}$ and $\Theta = \{A_1, A_2, \ldots, A_i\}$.

2.2. Basic Probability Assignment

For any proposition A in 2^{Θ}, $A \in 2^{\Theta}$, the function m is the mapping $2^{\Theta} \rightarrow [0,1]$ and m satisfies the following conditions.

$$\begin{cases} 0 \leq m(A) \leq 1 \\ m(\varnothing) = 0 \\ \sum_{A \subseteq \Theta} m(A) = 1 \end{cases} \tag{1}$$

Then, m is designated as the basic probability assignment (BPA) function on Θ, and $m(A)$ represents the BPA function of proposition A, commonly referred to as the mass

function. Proposition A is identified as a focal element if $m(A) > 0$. When all focal elements consist of singleton sets, such a focal element is termed a single-subset focal element evidence. Conversely, when the focal elements involve multi-subsets, it is denoted as multi-subset focal element evidence.

2.3. D-S Theory Synthesis Rules

Hypothesis m_1 and m_2 identify two independent BPA functions on the frame Θ. The combinatorial rule of the D-S evidence theory is defined as follows:

$$m(A) = m_1(A_i) \oplus m_2(A_j) = \begin{cases} 0, \ A = \varnothing \\ \frac{\sum_{A_i \cap A_j = A} m_1(A_i)m_2(A_j)}{1-k}, A \neq \varnothing \end{cases} \tag{2}$$

where $k = \sum_{A_i \cap A_j = \varnothing} m_1(A_i)m_2(A_j)$ stands for conflict degree and indicates the degree of conflict between two pieces of evidence, and $k \in [0, 1]$. The conflict coefficient is the greater degree of conflict between two pieces of evidence.

2.4. Belief Function and Plausibility Function

For proposition A, the belief function [32,33], denoted as Bel, is defined as follows:

$$\text{Bel}(A) = \sum_{A_i \subseteq A} m(A_i), \forall A_i \subseteq \Theta \tag{3}$$

The belief function represents the sum of the basic probability distribution functions for all subsets in proposition A, reflecting the minimum level of confidence in A. When A is a single-subset focal element, $\text{Bel}(A) = m(A)$.

For proposition A, the plausibility function Pls is defined as follows:

$$\text{Pls}(A) = 1 - \text{Bel}(\overline{A}) = \sum_{A_i \cap A \neq \varnothing} m(A_i), \forall A_i \subseteq \Theta \tag{4}$$

$\text{Pls}(A)$ denotes the highest level of trust in A, where $\text{Pls}(A) \geq \text{Bel}(A)$. The interval $[\text{Bel}(A), \text{Pls}(A)]$ represents the placement interval of proposition A. A wider placement interval indicates greater uncertainty about proposition A. When proposition A is a singleton set, $\text{Bel}(A) = \text{Pls}(A)$, signifying complete confidence in proposition A.

In evidence theory, uncertainty intervals emerge due to the presence of multi-set focal elements. As illustrated in Equation (4), when calculating the likelihood, each element assigns itself the exact value of the multi-subset focal element in which it is located. However, in the practical application of BPA, the value of the multi-subset focal element is collectively assigned by the elements that it contains. Therefore, the likelihood of each element should fall between $\text{Bel}(A)$ and $\text{Pls}(A)$, ensuring that the sum of the mass functions of all elements equals one. This compliance results in a probability function satisfying the following relation (5):

$$\begin{cases} \text{Bel}(A_i) \leq Probability(A_i) \leq \text{Pls}(A_i) \\ \sum_{A_i \subseteq \Theta} Probability(A_i) = 1 \end{cases} \tag{5}$$

3. Materials and Methods

3.1. Improved Pignistic Probability Function

When employing the BPA function to depict uncertain information regarding multi-subset focal elements, obtaining a precise decision directly from the BPA function becomes challenging. Typically, the BPA function of a multi-set focal element is viewed as supportive of a single-subset focal element, with a transformation of the BPA function from the multi-subset focal element into the decision probability distribution function of the single-subset focal element. To quantify this multi-subset focal element before reaching a decision, a probabilistic transformation method is applied. In the transferable belief model, Smets [34]

introduced the Pignistic probabilistic transformation method. The definition of the Pignistic probability transformation method is as follows:

$$BtPm(A_i) = \sum_{A_i \subseteq \Theta} \frac{|A_i \cap A|}{|A|} \frac{m(A)}{1 - m(\varnothing)} \tag{6}$$

where A is the subset of the identification frame Θ, $|\bullet|$ denotes the number of focal elements contained in the subset and $\varnothing$ is an empty set.

However, the conversion method proposed by Smets evenly distributes the values of multi-subset focal elements to the contained elements without fully considering the relationship between the evidence, making it less conducive to rational decision making.

Sudano and Martin [35] proposed an improved Pignistic probabilistic conversion method based on the difference in the credibility of multi-subset focal elements: the BPA of multi-subset focal elements is proportionally assigned to all Plausibilities (PraPl) based on the total likelihood of truth information of the single-subset focal elements. This significantly enhances the accuracy of the probabilistic conversion of multi-subset focal elements.

The PraPl probabilistic conversion method is defined as follows:

$$BetPm(A_i) = Bel(A_i) + \varepsilon\, Pls(A_i) \tag{7}$$

$$\varepsilon = \frac{1 - \sum_{A_i \subseteq \Theta} Bel(A_i)}{\sum_{A_i \subseteq \Theta} Pls(A_i)} \tag{8}$$

where $Pls(A_i)$ represents the plausibility function of A_i, and $Bel(A_i)$ is the belief function of A_i.

After conserving the improved Pignistic probability function, the BPA is converted into single subsets: $BetPm_1, BetPm_2, \ldots, BetPm_N$.

3.2. Evidence Similarity Based on the Bray–Curtis Dissimilarity

The Bray–Curtis dissimilarity [36], named after its originators J. Roger Bray and John T. Curtis, is primarily utilized in ecology and environmental sciences to measure the differences between samples and coordinate distances [37,38]. In this context, it serves to indicate the degree of support among evidence items.

For the sample space Θ, assuming two pieces of the evidence are m_i, m_j, the Bray–Curtis dissimilarity between them is given by the following:

$$b(m_i, m_j) = \frac{\sum_{k=1}^{M} \left| BetP_{m_i}(A_k) - BetP_{m_j}(A_k) \right|}{\sum_{k=1}^{M} BetP_{m_i}(A_k) + \sum_{k=1}^{M} BetP_{m_j}(A_k)} \tag{9}$$

where $i, j = 1, 2, \cdots, N$.

The Bray–Curtis dissimilarity, $i, j = 1, 2, \cdots, N$, between any two pieces of evidence can be represented by the matrix B, an N-dimensional matrix defined as follows:

$$B = \begin{bmatrix} b_{11} & b_{12} & \ldots & b_{1j} & \ldots & b_{1N} \\ b_{21} & b_{22} & \ldots & b_{2j} & \ldots & b_{2N} \\ \vdots & \vdots & \ddots & \vdots & \ddots & \vdots \\ b_{i1} & b_{i2} & \ldots & b_{ij} & \ldots & b_{iN} \\ \vdots & \vdots & \ddots & \vdots & \ddots & \vdots \\ b_{N1} & b_{N2} & \ldots & b_{Nj} & \ldots & b_{NN} \end{bmatrix} \tag{10}$$

where b_{ij} is $b(m_i, m_j)$ and represents the Bray–Curtis dissimilarity between evidence m_i and m_j. When $i = j$, $b_{ij} = 0$. The Bray–Curtis dissimilarity ranges between 0 and 1, with a

negative correlation indicating similarity with the evidence. Thus, the system's support for evidence is defined as follows:

$$sup(m_i) = \frac{1}{N-1} \sum_{j=1, j \neq i}^{N} \frac{1}{b_{ij}}$$

(11)

The weight of evidence m_i can be obtained after normalization as $wr_{(m_i)}$:

$$wr_{(m_i)} = \frac{sup(m_i)}{\sum_{j=1}^{N} sup(m_j)}$$

(12)

where $i = 1, 2, \cdots, N$.

3.3. Evidence Support Based on Cosine of the Included Angle

The consistency between evidence subjects can be established by determining the angle between two pieces of evidence. Furthermore, the similarity between the two subjects can be measured by the resulting angle. The formula for the cosine of the included angle is as follows [39,40]:

$$cos(m_i, m_j) = \frac{BetP_{m_i} \times BetP_{m_j}}{\|BetP_{m_i}\| \times \|BetP_{m_j}\|} = \frac{\sum_{k=1}^{M} BetP_{m_i}(A_k) \times BetP_{m_j}(A_k)}{\sqrt{\sum_{k=1}^{M} [BetP_{m_i}(A_k)]^2} \times \sqrt{\sum_{k=1}^{M} \left[BetP_{m_j}(A_k)\right]^2}}$$

(13)

Here, $\|BetP_{m_i}\|^2 = BetP_{m_i} \times BetP_{m_i}{}^T$; $\left\|BetP_{m_j}\right\|^2 = BetP_{m_j} \times BetP_{m_j}{}^T$; $i, j = 1, 2, \cdots, N$.

The pinch cosine distance between any two pieces of evidence can be expressed in the form of a pinch cosine similarity matrix D. The matrix D is an N-dimensional matrix defined as follows:

$$D = \begin{bmatrix} d_{11} & d_{12} & \dots & d_{1j} & \dots & d_{1N} \\ d_{21} & d_{22} & \dots & d_{2j} & \dots & d_{2N} \\ \vdots & \vdots & \ddots & \vdots & \ddots & \vdots \\ d_{i1} & d_{i2} & \dots & d_{ij} & \dots & d_{iN} \\ \vdots & \vdots & \ddots & \vdots & \ddots & \vdots \\ d_{N1} & d_{N2} & \dots & d_{Nj} & \dots & d_{NN} \end{bmatrix}$$

(14)

where d_{ij} is $cos(m_i, m_j)$, representing the cosine distance between evidence m_i and m_j. When $i = j$, $d_{ij} = 1$. The value range of the angle cosine distance is $[0, 1]$, which is positively correlated with the degree of similarity of the evidence, and therefore, the system's support for the evidence m_i is as follows:

$$sus(m_i) = \frac{1}{N-1} \sum_{j=1, j \neq i}^{N} d_{ij}$$

(15)

The weight of evidence m_i after normalization is denoted as $wt_{(m_i)}$:

$$wt_{(m_i)} = \frac{sus(m_i)}{\sum_{j=1}^{N} sus(m_j)}$$

(16)

where $i = 1, 2, \cdots, N$.

3.4. Evidence Uncertainty Based on Entropy

Entropy [41] is defined as the amount of information contained in the state that describes a random variable. Shannon [42] proposed Shannon entropy on the basis of information entropy, which was introduced into the D-S evidence theory to measure the

degree of uncertainty of evidence, while the belief entropy proposed by Deng [43] is a generalized improvement over Shannon entropy. Lower belief entropy indicates less information and uncertainty in the evidence, while higher belief entropy implies greater information and uncertainty.

This paper introduces belief entropy to quantify evidence uncertainty. Hypothesis m_i is a mass function defined on the frame of discernment Θ, $A_n(n = 1, 2, \cdots, N)$ is a proposition in mass function m_i, and $|A_n|$ is the cardinality of A_n. The belief entropy $H(m_i)$ regarding evidence m_i is given by the following [44,45]:

$$H(m_i) = - \sum_{A_n \subseteq \Theta} m_i(A_n) log_2 \frac{m_i(A_n)}{2^{|A_n|} - 1} \tag{17}$$

When the subset A_n contains only one element, denoted by $|A_n|$ = 1, the belief entropy degenerates into Shannon entropy:

$$H(m_i) = - \sum_{A_n \subseteq \Theta} m_i(A_n) log_2 m_i(A_n) \tag{18}$$

To prevent assigning zero weight to evidence m_i in certain cases, the paper determines the weight magnitude of evidence m_i by calculating the exponential form of the belief entropy:

$$U_i(m_i) = {}^{H(m_i)} = {}^{-\sum_{A_n \in \Theta} m_i(A_n) log_2 m_i(A_n)} \tag{19}$$

After normalization, the uncertainty of evidence m_i is computed as follows:

$$wn_{(m_i)} = \frac{U_{i(m_i)}}{\sum_{i=1}^{N} U_{i(m_i)}} \tag{20}$$

3.5. Evidence Fusion Based on the Dempster Rule

Based on the preceding analysis, the computation of the Bray–Curtis dissimilarity and the cosine of the included angle provides insight into evidence similarity, allowing for the determination of support degrees between evidence. A higher support degree corresponds to greater evidence credibility and results in a higher weighting coefficient. Simultaneously, evaluating the belief entropy of evidence reveals its uncertainty, with lower uncertainty signaling higher evidence credibility, meriting a greater weight. Integrating weights derived from the Bray–Curtis dissimilarity, cosine of the included angle distance, and belief entropy enhances the information impact on the evidence, assigning elevated weights to evidence with heightened credibility.

The weighted correction factor, considering evidence distance, evidence angle and uncertainty, for each piece of evidence is formulated as follows:

$$W_{i(m_i)} = wr_{(m_i)} \times wt_{(m_i)} \times wn_{(m_i)} \tag{21}$$

The weighted correction coefficients $W_{i(m_i)}$ are normalized to yield evidence fusion coefficients $W_{fus(m_i)}$:

$$W_{fus(m_i)} = \frac{W_{i(m_i)}}{\sum_{i=1}^{N} W_{i(m_i)}} \tag{22}$$

The mass function values of evidence m_i' are each assigned a corresponding weighted correction factor to obtain the corrected evidence m_i'':

$$m_i'' = \sum_{i=1}^{N} W_{fus(m_i)} \times m_i' \tag{23}$$

where $i = 1, 2, \cdots, n$. $N - 1$ fusion of m_i'' by the Dempster rule produces evidence fusion results in the following:

$$m_{fus} = \left(\left(\left(m_i'' \bigoplus m_i''\right)_1 \cdots\right)_i \bigoplus m_i''\right)_{N-1} \tag{24}$$

The presented flowchart illustrating the proposed method is depicted in Figure 1. Firstly, the original BPA function undergoes transformation into a singleton subset BPA function through the application of the improved Pignistic probability function. Secondly, a meticulous correction of weights is applied to conflicting evidence, focusing on three critical dimensions: evidence similarity, evidence distance and evidence uncertainty. This involves computing the support of each piece of evidence based on the Bray–Curtis dissimilarity, cosine of the included angle distance, and belief entropy, along with their respective weights. Thirdly, utilizing these three dimensions, the ultimate weighted correction coefficients for each piece of evidence are derived. These coefficients serve as the basis for the refinement of the singleton subset BPA function, resulting in the ultimate BPA function. Finally, the adjusted BPA function undergoes D-S evidence fusion, yielding the consolidated fusion results.
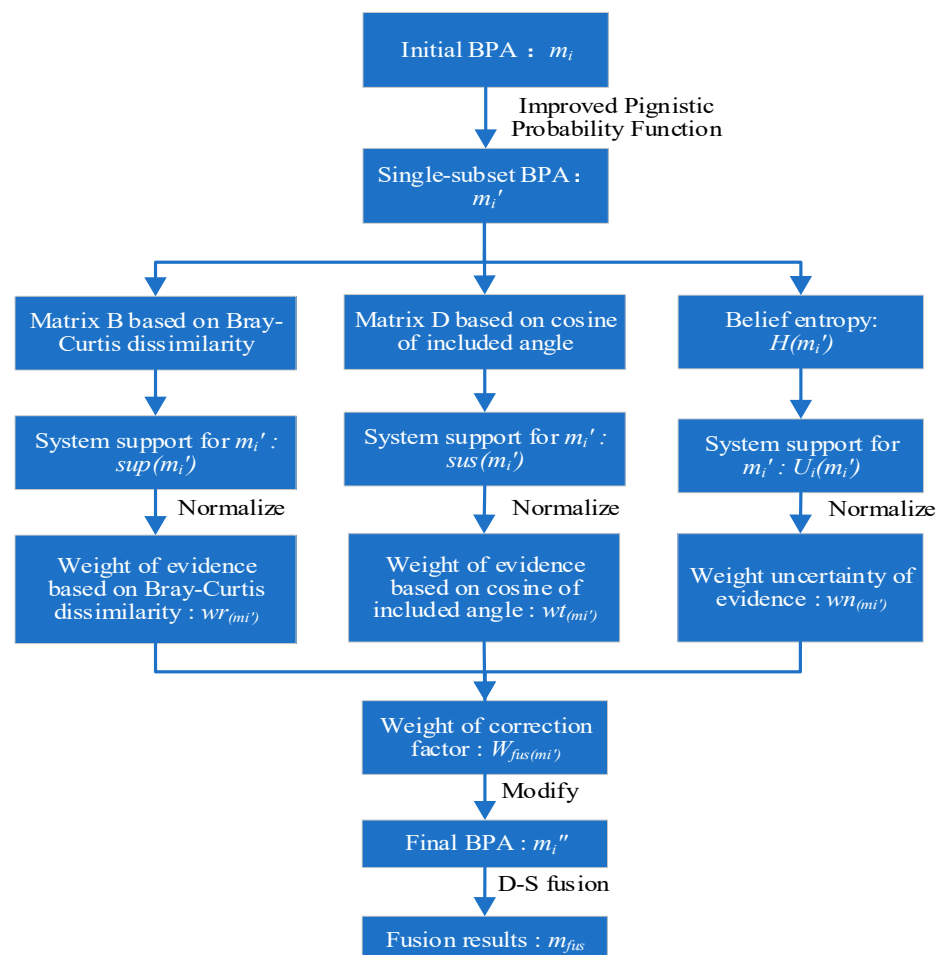

Figure 1. The flowchart of the proposed method.

The pseudocode for the proposed method is presented in Algorithm 1, outlining the approach for weighted fusion of conflicting evidence in this paper. The final fusion result of the collected evidence can be obtained by this algorithm to support decision making.

Assume a set of original evidence sources collected within the identification framework $\Theta = \{A_1, A_2, \cdots, A_N\}$, with the corresponding BPA function denoted as $m = \{m_1, m_2, \cdots, m_i\}$.

As depicted in Algorithm 1, lines 1–3 illustrate the process of converting collected BPA functions into a single subset of BPA functions, enhancing decision accuracy. Lines 4–12 elucidate the procedure for determining the weights of evidence similarity based on the Bray–Curtis dissimilarity. Subsequently, lines 13–21 detail the computation of evidence credibility weights using the cosine of the angle distance. Lines 22–27 articulate the methodology for assessing evidence uncertainty based on belief entropy. Further, lines 28–30 delineate the computation of the weighted fusion coefficients for evidence. Lines 31–33 expound on the correction of the original BPA function to yield the final BPA function value. Lastly, lines 34–36 explain the generation of fusion results.

Algorithm 1 Conflict Evidence Fusion Method Based on the Bray–Curtis Dissimilarity and the Belief Entropy

---

Input: Initial BPAs: $m = \{m_1, m_2, \cdots, m_i\}$
Output: Fusion Result: m_{fus}

1: *for $i = 1$; $i \leq N$ do*
2:    Applying Equations (7) and (8) for the initial BPA convert to single-subset BPA: m'_i;
3: *end*
4: *for $i = 1$; $i \leq N$ do*
5:    *for $j = 1$; $j \leq N$ do*
6:      Applying Equation (9) obtain Bray–Curtis dissimilarity between m'_i and m'_j: $b\left(m'_i, m'_j\right)$;
7:    *end*
8: *end*
9: Applying Equation (10) obtain Bray–Curtis dissimilarity matrix B;
10: *for $i = 1$; $i \leq N$ do*
11:   Applying Equations (11) and (12) obtain the weight of evidence based on Bray–Curtis dissimilarity: $wr(m_i\prime)$;
12: *end*
13: *for $i = 1$; $i \leq N$ do*
14:   *for $j = 1$; $j \leq N$ do*
15:     Applying Equation (13) obtain the cosine of included angle distance between m'_i and m'_j: $cos\left(m'_i, m'_j\right)$;
16:   *end*
17: *end*
18: Applying Equation (14) obtain the cosine of included angle distance matrix D;
19: *for $i = 1$; $i \leq N$ do*
20:   Applying Equations (15) and (16) obtain the weight of evidence based on cosine of included angle: wt($m_i\prime$);
21: *end*
22: *for $i = 1$; $i \leq N$ do*
23:   Applying Equations (17)–(19) obtain the Belief entropy: $H\left(m'_i\right)$;
24:   *end*
25: *for $i = 1$; $i \leq N$ do*
26:   Applying Equation (20) obtain the weight uncertainty of evidence: wn(m'_i);
27: *end*
28: *for $i = 1$; $i \leq N$ do*
29:   Applying Equations (21) and (22) obtain the evidence fusion coefficients: $W_{fus\,(m_i)}$;
30: *end*
31: *for $i = 1$; $i \leq N$ do*
32:   Applying Equation (23) obtain the final corrected BPA: m''_i;
33: *end*
34: *for $i = 1$; $i \leq N - 1$ do*
35:   Applying Equation (24) obtain the fusion result: m_{fus};
36: *end*

---

4. Experiments

To validate the effectiveness of the conflict evidence fusion method proposed in this paper, we reference two sets of classic conflict data. The first set comprises single-subset focal element data from the literature [26], while the second set consists of multiple subset focal element data sources from the literature [7]. These two sets of data sources have been widely employed in previous studies of enhanced methods and represent two forms of BPA functions. The application of the proposed fusion method to these two conflicting datasets, along with an analytical comparison against the D-S evidence theory and various improved fusion algorithms, serves to verify the efficiency and effectiveness of the method proposed in this paper.

4.1. An Example of Single-Subset Focal Element Data

There are five pieces of evidence on the frame of discernment $\Theta = \{A_1, A_2, A_3\}$, and the BPA function of each evidence is as follows:

$$m_1 : m_1(A_1) = 0.9, m_1(A_2) = 0, m_1(A_3) = 0.1;$$

$$m_2 : m_2(A_1) = 0, m_2(A_2) = 0.01, m_2(A_3) = 0.99;$$

$$m_3 : m_3(A_1) = 0.5, m_3(A_2) = 0.2, m_3(A_3) = 0.3;$$

$$m_4 : m_4(A_1) = 0.98, m_4(A_2) = 0.01, m_4(A_3) = 0.01;$$

$$m_5 : m_5(A_1) = 0.9, m_5(A_2) = 0.05, m_5(A_3) = 0.05.$$

Based on intuitive analysis, evidence m_1, m_3, m_4 and m_5 collectively supports proposition A_1, while evidence m_2 supports proposition A_3 with a higher degree of certainty, despite being conflicting evidence. The next step involves validation using the method proposed in this paper.

(1) Improved Pignistic probability function

The mass functions in the provided examples are all single-subset focal element evidential bodies. Consequently, the mass function values after conversion through the improved Pignistic probability function remain the same as the original BPA function values. The values of converted mass function are detailed in Table 1.

Table 1. The values of converted mass functions.

The Converted Mass Functions	$m'(A_1)$	$m'(A_2)$	$m'(A_3)$
m'_1	0.9	0	0.1
m'_2	0	0.01	0.99
m'_3	0.5	0.2	0.3
m'_4	0.98	0.01	0.01
m'_5	0.9	0.05	0.05

(2) The Bray–Curtis dissimilarity matrix is derived from Equations (9) and (10) as follows:

$$B = \begin{bmatrix} 0 & 0.9 & 0.4 & 0.09 & 0.05 \\ 0.9 & 0 & 0.69 & 0.98 & 0.94 \\ 0.4 & 0.69 & 0 & 0.43 & 0.38 \\ 0.09 & 0.98 & 0.43 & 0 & 0.08 \\ 0.05 & 0.94 & 0.38 & 0.08 & 0 \end{bmatrix}$$

Applying Equation (11), the evidence support based on the Bray–Curtis dissimilarity matrix is determined as follows:

$$sup(m'_i) = \{8.6806, 1.1612, 2.2266, 6.7393, 9.0489\}$$

Utilizing Equation (12) for normalization, the support coefficients become as follows:

$$wr_{(m_i')} = \{0.3116, 0.0417, 0.0799, 0.2419, 0.3248\}$$

(3) Equations (13) and (14) are applied to obtain the cosine distance matrix of the included angle:

$$D = \begin{bmatrix} 1 & 0.11 & 0.86 & 0.99 & 1.00 \\ 0.11 & 1 & 0.49 & 0.01 & 0.06 \\ 0.86 & 0.49 & 1 & 0.82 & 0.85 \\ 0.99 & 0.01 & 0.82 & 1 & 1.00 \\ 1.00 & 0.06 & 0.85 & 1.00 & 1 \end{bmatrix}$$

According to Equation (15), the similarity of the evidence available based on the cosine distance matrix of the included angle is determined as follows:

$$sus(m_i') = \{0.7400, 0.1675, 0.7550, 0.7050, 0.7275\}$$

Normalization of the evidence similarity coefficient according to Equation (16) results in the following:

$$wt_{(m_i')} = \{0.2391, 0.0541, 0.2439, 0.2278, 0.2351\}$$

(4) Applying Equations (17)–(19), the entropy of each evidence is calculated as follows:

$$U_i(m_i') = \{1.5984, 1.0841, 4.4171, 1.1752, 1.7665\}$$

Normalization of the evidence uncertainty coefficient according to Equation (20) yields the following:

$$wn_{(m_i')} = \{0.1592, 0.1080, 0.4399, 0.1170, 0.1759\}$$

(5) According to Equations (21)–(22), the normalized evidence weighted correction coefficient is calculated as follows:

$$W_{fus(m_i')} = \{0.2925, 0.0060, 0.2114, 0.1590, 0.3312\}$$

Applying Equation (23), a corresponding correction coefficient is assigned to each evidence, resulting in the final mass function value:

$$m_i'' = \sum_{i=1}^{N} W_{fus(m_i')} \times m_i' = \{0.8228, 0.0605, 0.1168\}$$

(6) Evidence fusion is executed according to Equation (24), and the final fusion results are presented in Table 2.

Table 2. Fusion results of single-subset focal element conflict data.

Fusion Results	$m(A_1)$	$m(A_2)$	$m(A_3)$
$m_1'' \oplus m_2''$	0.9751	0.0053	0.0196
$m_1'' \oplus m_2'' \oplus m_3''$	0.9968	0.0004	0.0029
$m_1'' \oplus m_2'' \oplus m_3'' \oplus m_4''$	0.9996	0.0000	0.0004
$m_1'' \oplus m_2'' \oplus m_3'' \oplus m_4'' \oplus m_5''$	0.9999	0.0000	0.0001

(7) Comparison with other improvement methods is outlined in Table 3. The variation in the mass function value of the proposition A_1 concerning different fusion rules and the number of fusions is illustrated in Figure 2.
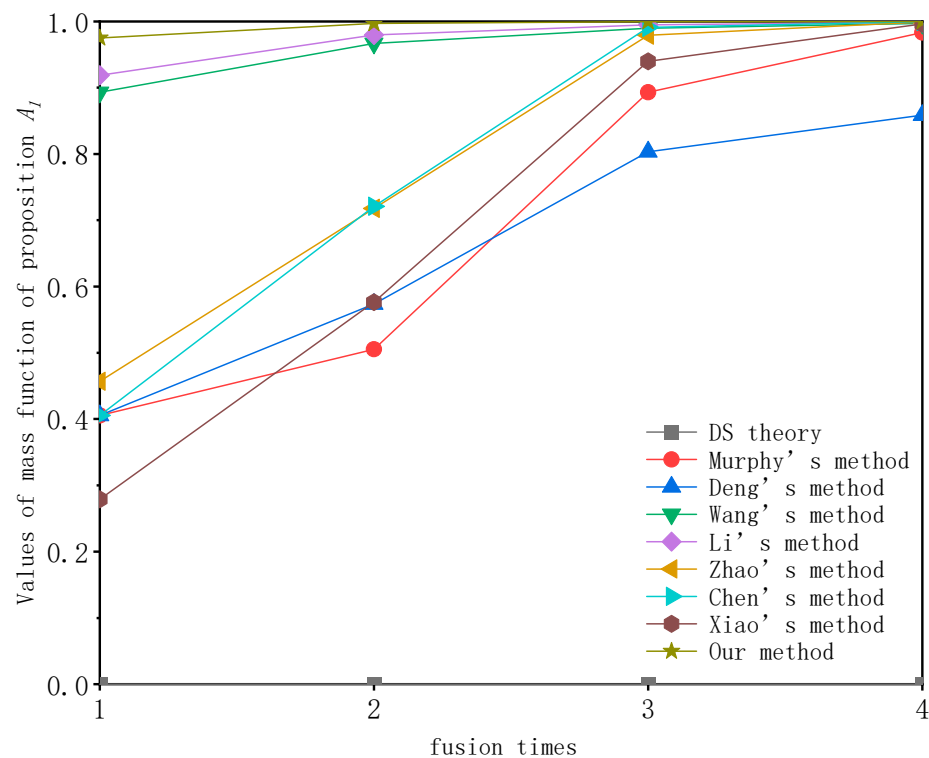
Figure 2. Mass function values of proposition A_1 for a single-subset of focal element conflict data under different fusion methods.

Table 3. Fusion results of single-subset focal element conflict data under various fusion methods.

Fusion Approach	BPA	First Fusion $m_1'' \oplus m_2''$	Second Fusion $m_1'' \oplus m_2'' \oplus m_3''$	Third Fusion $m_1'' \oplus m_2'' \oplus m_3'' \oplus m_4''$	Fourth Fusion $m_1'' \oplus m_2'' \oplus m_3'' \oplus m_4'' \oplus m_5''$
Dempster rule	$m(A_1)$	0.0000	0.0000	0.0000	0.0000
	$m(A_2)$	0.0000	0.0000	0.0000	0.0000
	$m(A_3)$	1.0000	1.0000	1.0000	1.0000
Murphy's method	$m(A_1)$	0.4054	0.5055	0.8930	0.9834
	$m(A_2)$	0.0001	0.0000	0.0001	0.0000
	$m(A_3)$	0.5946	0.4945	0.1069	0.0166
Deng's method	$m(A_1)$	0.4055	0.5737	0.8033	0.8585
	$m(A_2)$	0.0045	0.0866	0.0439	0.0379
	$m(A_3)$	0.5900	0.3397	0.1528	0.1036
Wang's method	$m(A_1)$	0.8931	0.9669	0.9898	0.9968
	$m(A_2)$	0.0179	0.0027	0.0004	0.0001
	$m(A_3)$	0.0890	0.3040	0.0098	0.0031
LI's method	$m(A_1)$	0.9189	0.9797	0.9949	0.9987
	$m(A_2)$	0.0180	0.0027	0.0004	0.0000
	$m(A_3)$	0.0630	0.0176	0.0047	0.0012
Zhao's method	$m(A_1)$	0.4571	0.7178	0.9792	0.9991
	$m(A_2)$	0.0000	0.0046	0.0001	0.0000
	$m(A_3)$	0.5429	0.2775	0.0207	0.0009
Chen's method	$m(A_1)$	0.4054	0.7211	0.9910	0.9996
	$m(A_2)$	0.0001	0.0040	0.0001	0.0000
	$m(A_3)$	0.5946	0.2749	0.0089	0.0003

Table 3. *Cont.*

Fusion Approach	BPA	First Fusion $m_1''\oplus m_2''$	Second Fusion $m_1''\oplus m_2''\oplus m_3''$	Third Fusion $m_1''\oplus m_2''\oplus m_3''\oplus m_4''$	Fourth Fusion $m_1''\oplus m_2''\oplus$ $m_3''\oplus m_4''\oplus m_5''$
Xiao's method	$m(A_1)$	0.2790	0.5763	0.9397	0.9963
	$m(A_2)$	0.0001	0.0065	0.0004	0.0000
	$m(A_3)$	0.7210	0.4173	0.0599	0.0037
Our method	$m(A_1)$	0.9751	0.9968	0.9996	0.9999
	$m(A_2)$	0.0053	0.0004	0.0000	0.0000
	$m(A_3)$	0.0196	0.0029	0.0004	0.0001

4.2. An Example of Multi-Subset Focal Element Data

There are five pieces of evidence on the frame of discernment $\Theta = \{A_1, A_2, A_3\}$, and the BPA function of each piece of evidence is, respectively, as follows:

$$m_1 : m_1(A_1) = 0.41, m_1(A_2) = 0.29, m_1(A_3) = 0.3;$$

$$m_2 : m_2(A_1) = 0, m_2(A_2) = 0.9, m_2(A_3) = 0.1;$$

$$m_3 : m_3(A_1) = 0.58, m_3(A_2) = 0.07, m_3(A_1, A_3) = 0.35;$$

$$m_4 : m_4(A_1) = 0.55, m_4(A_2) = 0.1, m_4(A_1, A_3) = 0.35;$$

$$m_5 : m_5(A_1) = 0.6, m_5(A_2) = 0.1, m_5(A_1, A_3) = 0.3.$$

Upon intuitive analysis, evidence m_1, m_3, m_4 and m_5 supports proposition A_1, while evidence m_2 supports proposition A_2 with a higher degree of certainty, despite being conflicting evidence. Validation is performed using the proposed method.

(1) Improved Pignistic probability function

For the multi-subset focal propositions m_3, m_4 and m_5, it is necessary to implement the improved Probabilistic transformations for their resolution.

According to Equations (3) and (4), the belief function and plausibility function values for m_3 are as follows:

$$\text{Bel}(A_1) = 0.58, \ \text{Bel}(A_2) = 0.07, \ \text{Bel}(A_3) = 0$$

$$\text{Pls}(A_1) = 0.93, \ \text{Pls}(A_2) = 0.07, \ \text{Pls}(A_3) = 0.35$$

According to Equations (7) and (8), the following holds:

$$\varepsilon = \frac{1 - \sum\limits_{A_i \subseteq \Omega} Bel(A_i)}{\sum\limits_{A_i \subseteq \Omega} Pls(A_i)} = 0.2593$$

$\text{BetPm}_3(A_1) = 0.8211$, $\text{BetPm}_3(A_2) = 0.0882$, and $\text{BetPm}_3(A_3) = 0.0908$.

Similarly, the following holds:

$\text{BetPm}_4(A_1) = 0.7834$, $\text{BetPm}_4(A_2) = 0.1259$, and $\text{BetPm}_4(A_3) = 0.0908$;

$\text{BetPm}_5(A_1) = 0.8077$, $\text{BetPm}_5(A_2) = 0.1231$, and $\text{BetPm}_5(A_3) = 0.0692$.

The values of mass function converted using the improved Pignistic probability function are shown in Table 4.

(2) The Bray–Curtis dissimilarity matrix, as derived from Equations (9) and (10), is represented by the following:

Table 4. Values of mass function after being converted.

The Converted Mass Functions	$m'(A_1)$	$m'(A_2)$	$m'(A_3)$
m'_1	0.4100	0.2900	0.3000
m'_2	0.0000	0.9000	0.1000
m'_3	0.8211	0.0882	0.0908
m'_4	0.7834	0.1259	0.0908
m'_5	0.8077	0.1231	0.0692

$$B = \begin{bmatrix} 0 & 0.6100 & 0.4110 & 0.3733 & 0.3977 \\ 0.6100 & 0 & 0.8210 & 0.7833 & 0.8077 \\ 0.4110 & 0.8210 & 0 & 0.0377 & 0.0349 \\ 0.3733 & 0.7833 & 0.0377 & 0 & 0.0243 \\ 0.3977 & 0.8077 & 0.0349 & 0.0243 & 0 \end{bmatrix}$$

Utilizing Equation (11), the support of the evidence based on the Bray–Curtis dissimilarity matrix is computed as follows:

$$sup(m'_i) = \{2.3164, 1.3430, 14.7074, 17.9082, 18.3895\}$$

After normalization according to Equation (12), the coefficients of support for the evidence are as follows:

$$wr(m'_i) = \{0.0424, 0.0246, 0.2690, 0.3276, 0.3364\}$$

(3) The cosine distance matrix of the included angle, obtained from Equations (13) and (14), is given by the following:

$$D = \begin{bmatrix} 1 & 0.5493 & 0.8014 & 0.8240 & 0.8081 \\ 0.5493 & 1 & 0.1176 & 0.1692 & 0.1585 \\ 0.8014 & 0.1176 & 1 & 0.9986 & 0.9987 \\ 0.8240 & 0.1692 & 0.9986 & 1 & 0.9995 \\ 0.8081 & 0.1585 & 0.9987 & 0.9995 & 1 \end{bmatrix}$$

According to Equation (15), the similarity of the evidence based on the cosine distance matrix is as follows:

$$sus(m'_i) = \{0.7457, 0.2487, 0.7291, 0.7478, 0.7412\}$$

The normalized evidence similarity coefficient according to Equation (16) is as follows:

$$wt(m'_i) = \{0.2321, 0.0774, 0.2270, 0.2328, 0.2307\}$$

(4) Applying Equations (17)–(19), the entropy of each available evidence is determined as follows:

$$U_i(m'_i) = \{4.7893, 1.5984, 2.3555, 2.6289, 2.4291\}$$

The coefficient of uncertainty of evidence after normalization according to Equation (20) is as follows:

$$wn(m'_i) = \{0.3470, 0.1158, 0.1707, 0.1905, 0.1760\}$$

(5) According to Equations (21)–(22), the normalized evidence weighted correction coefficient is obtained as follows:

$$W_{fus(m'_i)} = \{0.0808, 0.0052, 0.2467, 0.3439, 0.3234\}$$

According to Equation (23), each piece of evidence is assigned a corresponding correction coefficient, and the resulting mass function value can be calculated as follows:

$$m_i'' = \sum_{i=1}^{N} W_{fus(m_i')} \times m_i' = \{0.7633,\ 0.1330,\ 0.1008\}$$

(6) Convergence of Evidence Based on D-S Theory

Evidence fusion is carried out according to Equation (24), and the final fusion results are shown in Table 5.

Table 5. Fusion results of multi-subset focal element conflict data.

Fusion Results	$m(A_1)$	$m(A_2)$	$m(A_3)$
$m1'' \oplus m2''$	0.9547	0.0288	0.0165
$m1'' \oplus m2'' \oplus m3''$	0.9926	0.0052	0.0023
$m1'' \oplus m2'' \oplus m3'' \oplus m4''$	0.9988	0.0009	0.0003
$m1'' \oplus m2'' \oplus m3'' \oplus m4'' \oplus m5''$	0.9998	0.0002	0.0000

(7) Comparison with alternative improvement methods is illustrated in Table 6. The variations in the mass function value of the proposition A_1 across different fusion rules and fusion numbers are depicted in Figure 3.
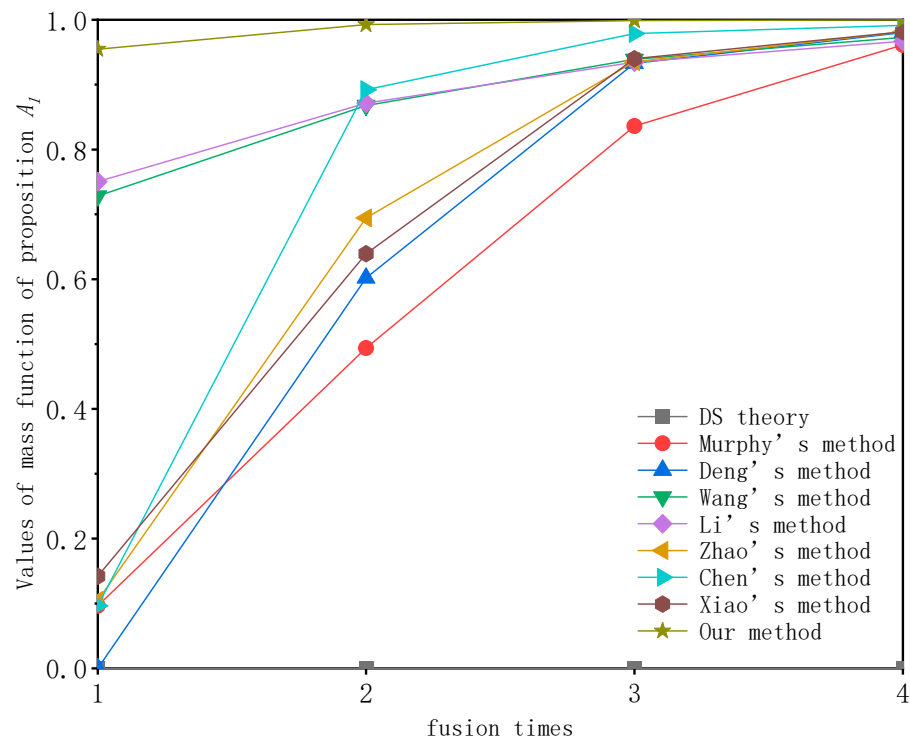

Figure 3. Change in mass function value of proposition A_1 under varying fusion rules and fusion numbers.

Table 6. Fusion results of multi-subset focal element conflict data under different fusion methods.

Fusion Approach	BPA	First Fusion $m_1''\oplus m_2''$	Second Fusion $m_1''\oplus m_2''\oplus m_3''$	Third Fusion $m_1''\oplus m_2''\oplus m_3''\oplus m_4''$	Fourth Fusion $m_1''\oplus m_2''\oplus$ $m_3''\oplus m_4''\oplus m_5''$
Dempster rule	$m(A_1)$	0.0000	0.0000	0.0000	0.0000
	$m(A_2)$	0.8969	0.6350	0.3320	0.0000
	$m(A_3)$	0.1031	0.3650	0.6680	1.0000
Murphy's method	$m(A_1)$	0.0964	0.4939	0.8362	0.9613
	$m(A_2)$	0.8119	0.4180	0.1147	0.0147
	$m(A_3)$	0.0917	0.0792	0.0410	0.0166
	$m(A_1, A_3)$	0.0000	0.0090	0.0081	0.0032
Deng's method	$m(A_1)$	0.0000	0.6019	0.9329	0.9802
	$m(A_2)$	0.8969	0.2908	0.0225	0.0009
	$m(A_3)$	0.1031	0.0991	0.0354	0.0154
	$m(A_1, A_3)$	0.0000	0.0082	0.0092	0.0035
Wang's method	$m(A_1)$	0.7283	0.8679	0.9393	0.9728
	$m(A_2)$	0.0972	0.0423	0.0167	0.0063
	$m(A_3)$	0.0180	0.0034	0.0006	0.0000
	$m(A_1, A_3)$	0.1565	0.0865	0.0433	0.0208
LI's method	$m(A_1)$	0.7505	0.8714	0.9346	0.9669
	$m(A_2)$	0.0504	0.0152	0.0042	0.0011
	$m(A_3)$	0.0072	0.0008	0.0000	0.0000
	$m(A_1, A_3)$	0.1918	0.1126	0.0610	0.0319
Zhao's method	$m(A_1)$	0.1046	0.6945	0.9355	0.9817
	$m(A_2)$	0.7989	0.1902	0.0163	0.0000
	$m(A_3)$	0.0965	0.1062	0.0409	0.0147
	$m(A_1, A_3)$	0.0000	0.0091	0.0073	0.0036
Chen's method	$m(A_1)$	0.0964	0.8923	0.9788	0.9916
	$m(A_2)$	0.8119	0.0293	0.0010	0.0001
	$m(A_3)$	0.0917	0.0455	0.0102	0.0026
	$m(A_1, A_3)$	0.0000	0.0329	0.0173	0.0057
Xiao's method	$m(A_1)$	0.1420	0.6391	0.9400	0.9816
	$m(A_2)$	0.7412	0.2462	0.0165	0.0006
	$m(A_3)$	0.1168	0.1072	0.0341	0.0141
	$m(A_1, A_3)$	0.0000	0.0075	0.0093	0.0037
Our method	$m(A_1)$	0.9547	0.9926	0.9988	0.9998
	$m(A_2)$	0.0288	0.0052	0.0009	0.0002
	$m(A_3)$	0.0165	0.0023	0.0003	0.0000

4.3. Discussion

In this section, we present two approaches for fusing conflicting evidence from single-subset and multi-subset focal element data sources. Initially, the effectiveness of the improved Pignistic probability function is validated. Leveraging the total likelihood of truth information from single-subset focal elements, the evidence from multi-subset focal elements is allocated to single-subset propositions based on confidence intervals. This approach maximizes the utilization of existing information, enabling the rapid identification of the correct proposition A_1, even in the presence of conflicting data sources from multi-subset focal elements.

As shown in Figure 2 and Table 3, when validating conflict data with singleton focal elements, the D-S evidence theory fails to correctly identify the proposition A_1. Notably, the methods proposed by Xiao, Murphy, Zhao and Chen in their first fusion attempts all yielded mass function values for the proposition A_1 that did not surpass 0.5. In contrast, our proposed method achieved a substantial improvement, reaching a mass function value of 0.9751 for the proposition A_1 in the first fusion iteration, outperforming all of the aforementioned methods. With increasing fusion iterations, the mass function value

for the proposition A_1 steadily increased, reaching 0.9999 in the final fusion iteration, consistently surpassing the fusion accuracy of the aforementioned improved methods. Compared to Murphy's method, our proposed method exhibited a 1.68% improvement, a 0.36% improvement over Xiao's method and a 0.03% improvement over Chen's method.

As illustrated in Figure 3 and Table 6, when validating conflict data with multiple subset focal elements, the D-S evidence theory still failed to identify the correct proposition A_1. Deng and Chen's methods, in their initial fusion attempts, both failed to correctly identify A_1. For Murphy, Zhao and Xiao's methods, the mass function values for proposition A_1 did not exceed 0.2 in the first fusion iteration. In contrast, our proposed method achieved a mass function value of 0.9547 for the proposition A_1 in the first fusion iteration, reaching 0.9998 in the final fusion iteration. This consistently exceeded the fusion accuracy of the aforementioned improved methods, showing a 4% improvement over Murphy's method, a 1.86% improvement over Xiao's method and a 0.83% improvement over Chen's method.

In summary, our proposed method demonstrates faster convergence and higher fusion accuracy compared to previously proposed improved methods. This validates the effectiveness and feasibility of the proposed approach.

5. Conclusions

This paper conducts a comprehensive study on conflict issues in evidence fusion, proposing the use of the improved Pignistic probability function to convert multi-subset focal element evidence into single-subset focal element evidence. This approach enhances the universality of conflict data fusion methods. The novel combination of the Bray–Curtis dissimilarity and cosine of the included angle distance is introduced as a means to measure evidence credibility. This, coupled with the belief entropy metric, gauges evidence uncertainty and determines the final weighting correction coefficients for the evidence. In the validation of conflicting evidence, the results demonstrate that the proposed method can rapidly and effectively identify target propositions. It exhibits faster convergence speed, higher fusion accuracy and better performance in addressing evidence conflict challenges.

Author Contributions: Conceptualization, Y.L.; methodology, Y.L. and T.Z.; validation, Y.L. and T.Z.; data curation, Y.L.; writing—original draft preparation, Y.L.; writing—review and editing, T.Z. and H.F. All authors have read and agreed to the published version of the manuscript.

Data Availability Statement: No new data were created or analyzed in this study.

Conflicts of Interest: The authors declare no conflicts of interest.

References

1. Dempster, A.P. Upper and Lower Probabilities Induce by a Multiplicand Mapping. *Ann. Math. Stat.* **1967**, *38*, 325–339. [CrossRef]
2. Glenn, S. *A Mathematical Theory of Evidence*; Princeton University Press: Princeton, NJ, USA, 1976; Volume 42.
3. Basir, O.; Yuan, X. Engine fault diagnosis based on multi-sensor information fusion using Dempster–Shafer evidence theory. *Inf. Fusion* **2007**, *8*, 379–386. [CrossRef]
4. Zhang, X.; Ma, Y.; Li, Y.; Zhang, C.; Jia, C. Tension prediction for the scraper chain through multi-sensor information fusion based on improved Dempster-Shafer evidence theory. *Alex. Eng. J.* **2023**, *64*, 41–54. [CrossRef]
5. Belmahdi, F.; Lazri, M.; Ouallouche, F.; Labadi, K.; Absi, R.; Ameur, S. Application of Dempster-Shafer theory for optimization of precipitation classification and estimation results from remote sensing data using machine learning. *Remote Sens. Appl. Soc. Environ.* **2023**, *29*, 100906. [CrossRef]
6. Hamid, R.A.; Albahri, A.S.; Albahri, O.S.; Zaidan, A.A. Dempster–Shafer theory for classification and hybridised models of multi-criteria decision analysis for prioritisation: A telemedicine framework for patients with heart diseases. *J. Ambient. Intell. Humaniz. Comput.* **2022**, *13*, 4333–4367. [CrossRef]
7. Chen, L.; Diao, L.; Sang, J. Weighted evidence combination rule based on evidence distance and uncertainty measure: An application in fault diagnosis. *Math. Probl. Eng.* **2018**, *2018*, 5858272. [CrossRef]
8. Ghosh, N.; Saha, S.; Paul, R. iDCR: Improved Dempster Combination Rule for multisensor fault diagnosis. *Eng. Appl. Artif. Intell.* **2021**, *104*, 104369. [CrossRef]
9. Fei, L.; Wang, Y. An optimization model for rescuer assignments under an uncertain environment by using Dempster–Shafer theory. *Knowl.-Based Syst.* **2022**, *255*, 109680. [CrossRef]

10. Fei, L.; Feng, Y. Modeling interactive multiattribute decision-making via probabilistic linguistic term set extended by Dempster–Shafer theory. *Int. J. Fuzzy Syst.* **2021**, *23*, 599–613. [CrossRef]

11. Jia, R.S.; Liu, C.; Sun, H.M.; Yan, X.H. A situation assessment method for rock burst based on multi-agent information fusion. *Comput. Electr. Eng.* **2015**, *45*, 22–32. [CrossRef]

12. Liu, Z.G.; Pan, Q.; Dezert, J.; Martin, A. Adaptive imputation of missing values for incomplete pattern classification. *Pattern Recognit.* **2016**, *52*, 85–95. [CrossRef]

13. Zadeh, L.A. Review of a mathematical theory of evidence. *AI Mag.* **1984**, *5*, 81.

14. Cuzzolin, F. A geometric approach to the theory of evidence. *IEEE Trans. Syst. ManCybern. Part C (Appl. Rev.)* **2008**, *38*, 522–534. [CrossRef]

15. Yager, R.R. On the Dempster-Shafer framework and new combination rules. *Inf. Sci.* **1987**, *41*, 93–137. [CrossRef]

16. Florea, M.C.; Jousselme, A.L.; Bossé, É.; Grenier, D. Robust combination rules for evidence theory. *Inf. Fusion* **2009**, *10*, 183–197. [CrossRef]

17. Su, X.; Li, L.; Qian, H.; Mahadevan, S.; Deng, Y. A new rule to combine dependent bodies of evidence. *Soft Comput.* **2019**, *23*, 9793–9799. [CrossRef]

18. Murphy, C.K. Combining belief functions when evidence conflicts. *Decis. Support Syst.* **2000**, *29*, 1–9. [CrossRef]

19. Yong, D.; Shi, W.; Zhu, Z.; Liu, Q. Combining belief functions based on distance of evidence. *Decis. Support Syst.* **2004**, *38*, 489–493. [CrossRef]

20. Lin, Y.; Wang, C.; Ma, C.; Dou, Z.; Ma, X. A new combination method for multisensor conflict information. *J. Supercomput.* **2016**, *72*, 2874–2890. [CrossRef]

21. Shi, X.; Liang, F.; Qin, P.; Yu, L.; He, G. A Novel Evidence Combination Method Based on Improved Pignistic Probability. *Entropy* **2023**, *25*, 948. [CrossRef]

22. Tang, Y.; Dai, G.; Zhou, Y.; Huang, Y.; Zhou, D. Conflicting evidence fusion using a correlation coefficient-based approach in complex network. *Chaos Solitons Fractals* **2023**, *176*, 114087. [CrossRef]

23. Xiao, F. Multi-sensor data fusion based on the belief divergence measure of evidences and the belief entropy. *Inf. Fusion* **2019**, *46*, 23–32. [CrossRef]

24. Zhao, K.; Sun, R.; Li, L.; Hou, M.; Yuan, G.; Sun, R. An improved evidence fusion algorithm in multi-sensor systems. *Appl. Intell.* **2021**, *51*, 7614–7624. [CrossRef]

25. Li, J.; Xie, B.; Jin, Y.; Hu, Z.; Zhou, L. Weighted conflict evidence combination method based on Hellinger distance and the belief entropy. *IEEE Access* **2020**, *8*, 225507–225521. [CrossRef]

26. Wang, X.; Di, P.; Yin, D. Conflict evidence fusion method based on lance distance and credibility entropy. *Syst. Eng. Electron.* **2021**, *44*, 592–602. [CrossRef]

27. Zhou, C.; Xu, D.; Cao, Z. Conflict evidence fusion method for single subset focus elements. *J. Beijing Univ. Aeronaut. Astronaut.* **2023**, 1–11. [CrossRef]

28. Zhang, H.; Lu, J.; Tang, X. An improved DS evidence theory algorithm for conflict evidence. *J. Beijing Univ. Aeronaut. Astronaut.* **2020**, *46*, 616–623.

29. Pal, N.R.; Bezdek, J.C.; Hemasinha, R. Uncertainty measures for evidential reasoning I: A review. *Int. J. Approx. Reason.* **1992**, *7*, 165–183. [CrossRef]

30. George, T.; Pal, N.R. Quantification of conflict in Dempster-Shafer framework: A new approach. *Int. J. Gen. Syst.* **1996**, *24*, 407–423. [CrossRef]

31. Lefevre, E.; Colot, O.; Vannoorenberghe, P.; De Brucq, D. A generic framework for resolving the conflict in the combination of belief structures. In Proceedings of the Third International Conference on Information Fusion, Paris, France, 10–13 July 2000; IEEE: Piscataway, NJ, USA, 2000.

32. Pan, W.; Wang, Y.; Yang, H. Design of Pignistic probability conversion algorithm. *Comput. Eng.* **2005**, *31*, 20–22+25.

33. Dubois, D.; Prade, H. Representation and combination of uncertainty with belief functions and possibility measures. *Comput. Intell.* **1988**, *4*, 244–264. [CrossRef]

34. Smets, P.; Kennes, R. The transferable belief model. *Class. Work. Dempster-Shafer Theory Belief Funct.* **2008**, *2019*, 693–736.

35. Sudano, J.J. Pignistic probability transforms for mixes of low-and high-probability events. *arXiv* **2015**, arXiv:1505.07751.

36. Bray, J.R.; Curtis, J.T. An ordination of the upland forest communities of southern Wisconsin. *Ecol. Monogr.* **1957**, *27*, 326–349. [CrossRef]

37. Ricotta, C.; Podani, J. On some properties of the Bray-Curtis dissimilarity and their ecological meaning. *Ecol. Complex.* **2017**, *31*, 201–205. [CrossRef]

38. Ricotta, C.; Pavoine, S. A new parametric measure of functional dissimilarity: Bridging the gap between the Bray-Curtis dissimilarity and the Euclidean distance. *Ecol. Model.* **2022**, *466*, 109880. [CrossRef]

39. Wen, C.; Wang, Y.; Xu, X. Fuzzy information fusion algorithm of fault diagnosis based on similarity measure of evidence. In *Advances in Neural Networks-ISNN 2008, Proceedings of the 5th International Symposium on Neural Networks, ISNN 2008, Beijing, China, 24–28 September 2008*; Springer: Berlin/Heidelberg, Germany, 2008; Volume 5, pp. 506–515.

40. Chen, B.C.; Tao, X.; Yang, M.R.; Yu, C.; Pan, W.M.; Leung, V.C. A saliency map fusion method based on weighted DS evidence theory. *IEEE Access* **2018**, *6*, 27346–27355. [CrossRef]

41. Khan, M.N.; Anwar, S. Paradox elimination in Dempster–Shafer combination rule with novel entropy function: Application in decision-level multi-sensor fusion. *Sensors* **2019**, *19*, 4810. [CrossRef]
42. Shannon, C.E. A mathematical theory of communication. *ACM SIGMOBILE Mob. Comput. Commun. Rev.* **2001**, *5*, 3–55. [CrossRef]
43. Deng, Y. Deng Entropy: A generalized Shannon Entropy to Measure Uncertainty. Available online: https://fs.unm.edu/DengEntropyAGeneralized.pdf (accessed on 31 January 2015).
44. Yan, H.; Deng, Y. An improved belief entropy in evidence theory. *IEEE Access* **2020**, *8*, 57505–57516. [CrossRef]
45. Yuan, K.; Xiao, F.; Fei, L.; Kang, B.; Deng, Y. Conflict management based on belief function entropy in sensor fusion. *SpringerPlus* **2016**, *5*, 638. [CrossRef] [PubMed]